European Journal of Engineering Science and Technology
ISSN 2538-9181

Effect of Twin Circular Underground Voids on Bearing Capacity of Strip Foundations

Javad Mofidi Rouchi[1*], and Mohammad Amin Nozari[2]

[1] Department of Civil, Materials, and Environmental Engineering, University of Illinois Chicago, USA
[2] Deptartment of Civil and Environmental Engineering, University of Delaware, USA

ARTICLE INFO

Keywords:
twin voids,
bearing capacity,
lower bound,
finite element method

ABSTRACT

Underground voids can significantly alter the stress and strain conditions of the surrounding soil mass, consequently affecting the stability of buildings located on the surface. Numerous numerical and experimental methods have been employed to investigate the effects of voids on nearby structures. In this research, a mixed lower bound-finite element method is utilized to study the stability of strip foundations situated above twin continuous voids. The soil behavior is modeled using the Mohr-Coulomb yield function along with an associated flow rule. Three-noded triangular stress elements are used to mesh the stress field, considering stress discontinuities at the common edges of adjacent elements. The study assumes that the two voids are identical in terms of radius, distance from the footing centerline, and depth from the ground level. The primary geometrical parameters considered in the analysis are the location and radius of the voids, as well as the strength parameters of the soil. By investigating the changes in bearing capacity concerning these factors, practical charts are proposed to aid in understanding the stability of the foundation. The results of the current study reveal the existence of an unsafe zone beneath the foundations, where the impact of the twin voids on bearing capacity reduction can be significant. Understanding these effects is crucial for design and construction of structures in areas prone to underground voids and also to decide where to bore infrastructure tunnels in order to have minimum effect on stability of the above buildings.

1. Introduction

Underground voids can be created in urban areas by various reasons such as infrastructures conduits, tunneling, abandoned or forgotten structures, utility conduits and pipelines. The effect of voids on the bearing capacity of foundation has been studied over several years and it plays major role in foundation engineering problems. Miscellaneous methods such as Analytical, Experimental and Numerical studies have been conducted to know the behavior of footings due to presence of voids. Numerical methods enable engineers to evaluate the response of buildings and structures to the presence of underground voids. By utilizing these methods,

* Corresponding Author E-Mail Address: jmofid2@uic.edu

Cite this article as:
Mofidi Rouchi, J., & Nozari, M. A. (2023). Effect of Twin Circular Underground Voids on Bearing Capacity of Strip Foundations. *European Journal of Engineering Science and Technology*, *6*(2): 1-13. https://doi.org/10.33422/ejest.v6i2.1137

engineers can assess the stability, identify potential failure mechanisms, and design appropriate mitigation measures to ensure the safety and serviceability of the structure. Badie et.al. (1984) investigated stability of spread footing over continuous voids by both analytical and experimental methods. Thomas & Billy (1987) developed a mathematical model to design the road embankments with geosynthetics over voids and presented comparison results by performing various field tests to verify developed mathematical model. Wang et.al. (1987) developed a rational method for stability of footing, complex equations relating the maximum footing pressure and other influencing factors such as void size, location of void and soil strength property. Azam et.al. (1991) investigated the behaviour of strip footing over void supported by a homogeneous soil of finite thickness and a stratified deposit containing two layers. Kiyosumi et.al.(2007) developed a calculation formula for estimating the yielding pressure of strip footing above multiple voids numerically using two dimensional plane strain finite element analysis. Sireesh et.al. (2009) conducted model tests to investigate the benefits of provision of geocell reinforced sand mattress over clay with void. Kiyosumi et. al. (2011) were conducted a series of loading tests on shallow foundation of sedimentary rock considering square and rectangular voids. Sabouni (2013) examined the effect of single and double voids on the settlement and effective stresses underneath the strip footing numerically through parametric study. Joon et.al. (2014) investigated the undrained vertical bearing capacity of strip footing on clay with single and double voids. The undrained bearing capacity factors were determined using design charts by means of finite element analysis. Wilson et al. (2014) used numerical limit analysis to investigate the effect of the tunnel spacing on the stability of two circular tunnels excavated side by side. Yan-Jun et al. (2019) investigated the effects of twin tunnels on existing building foundations with a case study of Guanyinqiao subway station. By combining field monitoring data with numerical simulations, their study contributes to a better understanding of the effects of twin tunnels on existing buildings, aiding in the design and management of similar projects in urban areas. Naveen et al. (2017) focused on investigating the impact of twin tunnel construction on existing buildings with piled foundations. They utilized finite element analysis to study the behavior of adjacent buildings during the construction phase of twin tunnels. They simulated the construction process and analyzed the structural behavior, including settlements and stresses induced in the buildings and piles due to tunneling construction. In current study, the lower bound limit analysis and finite element methods are combined together to investigate the effects of twin underground voids on bearing capacity of shallow foundations. This method enables the engineers to estimate the lower limit of foundation load which leads to a safe and also more conservative stability design of foundations. For a particular range of parameters, the reducing effect of voids is scrutinized and applicable charts are presented.

2. Problem Definition

The problem of a strip footing above the twin circular underground voids is shown in Figure 1. Geometric parameters include the footing width B, the voids diameters D, the net horizontal distance between the voids d and the thickness of soil above the voids crest h. The voids are twin with same diameters, same distance from the footing centerline and same depth from the ground level. It is assumed that the soil obeys the associated flow rule with the Mohr-Coulomb yield criterion and has the cohesion of c, internal friction angle of ϕ and unit weight of γ. The voids are assumed to be bare and without any facing with no internal pressure. The lower bound limit load (P) then can be computed throughout the admissible stress field.

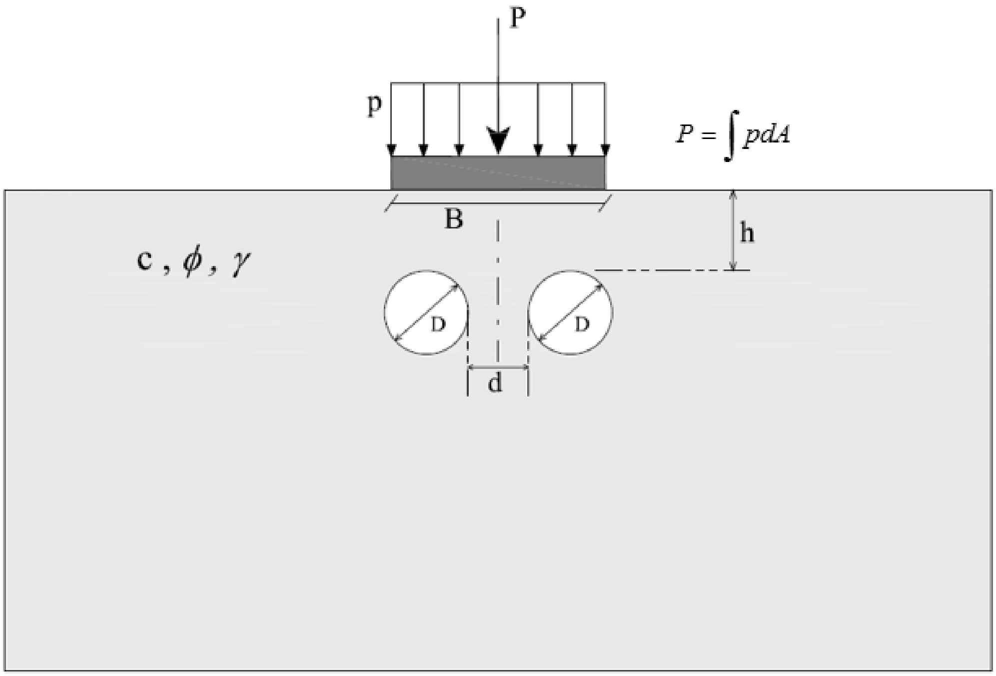

Figure 1. Problem parameters

The normalized lower bound pressure under the footing base can be defined as a relevant dimensionless geometrical parametetrs and soil strength parameters as:

$$\frac{p}{\gamma B} = f\left(\frac{d}{B}, \frac{h}{B}, \frac{D}{B}, c, \phi\right) \tag{1}$$

3. Finite Element Formulation of Lower Bound Limit Analysis

The lower bound theorem of limit analysis can be stated as follows (Chen, 1975):

“ If for a given load factor $\tilde{\lambda}$ the stress field (i) satisfies the stress boundary conditions, (ii) is in static equilibrium and (iii) does not violate the yield condition, then the load factor is a lower bound of the collapse load, i.e. $\tilde{\lambda} \leq \lambda^*$ and the stress field is called a statically admissible stress field.“

The aim of lower bound theory is to maximize the integral below which is called objective function in mathematics terminology:

$$P = \int_{A_p} pdA \tag{2}$$

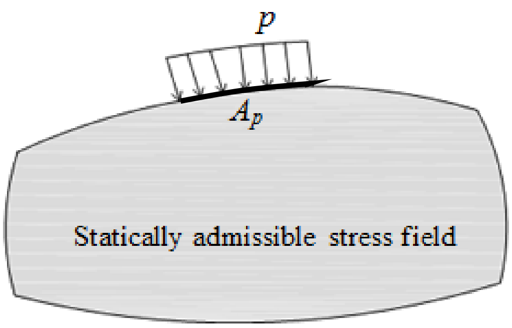

Figure 2. Lower bound limit pressure

in which p is the unknown traction acting on the surface area A_p (Figure 2).

By assembling all equalities and inequalities, discrete formulation of the lower bound theory leads to following constrained optimization problem:

maximize $P(\mathbf{x})$

$$\text{subjtected to} \quad \begin{cases} f_i(\mathbf{x}) = 0 \quad , \quad i \in I = \{1, \ldots, m\} \\ g_j(\mathbf{x}) \le 0 \quad , \quad j \in J = \{1, \ldots, n\} \end{cases} \tag{3}$$

where P is the collapse load, $\mathbf{x}$ is the vector of problem unknowns, f_i are the equality functions derived from element equilibrium, discontinuity equilibrium and boundary conditions, while g_j are inequality functions derived from yield criterion and other inequality constraints.

The formulation used in this paper follows that of Sloan (1988) in which the linear finite element method is applied and the domain of problem is discretized by 3-noded triangular elements. Unknowns of the problem are nodal stresses (σ_x, σ_y, τ_{xy}). The main difference between lower bound mesh and usual finite element mesh is that some nodes may have the same coordinate. Thus, the statically admissible stress discontinuities can occur at shared edges of adjacent elements (Figure 3b). By using linear finite elements and linearized yield function, the lower estimation of true collapse load can be obtained through linear programming techniques. As Lyamin & Sloan (2002) discussed elaborately, using linear finite elements is the most appropriate way for discretizing the domain of the problem in lower bound theory. In this way, the stresses vary linearly along the sides of each element.

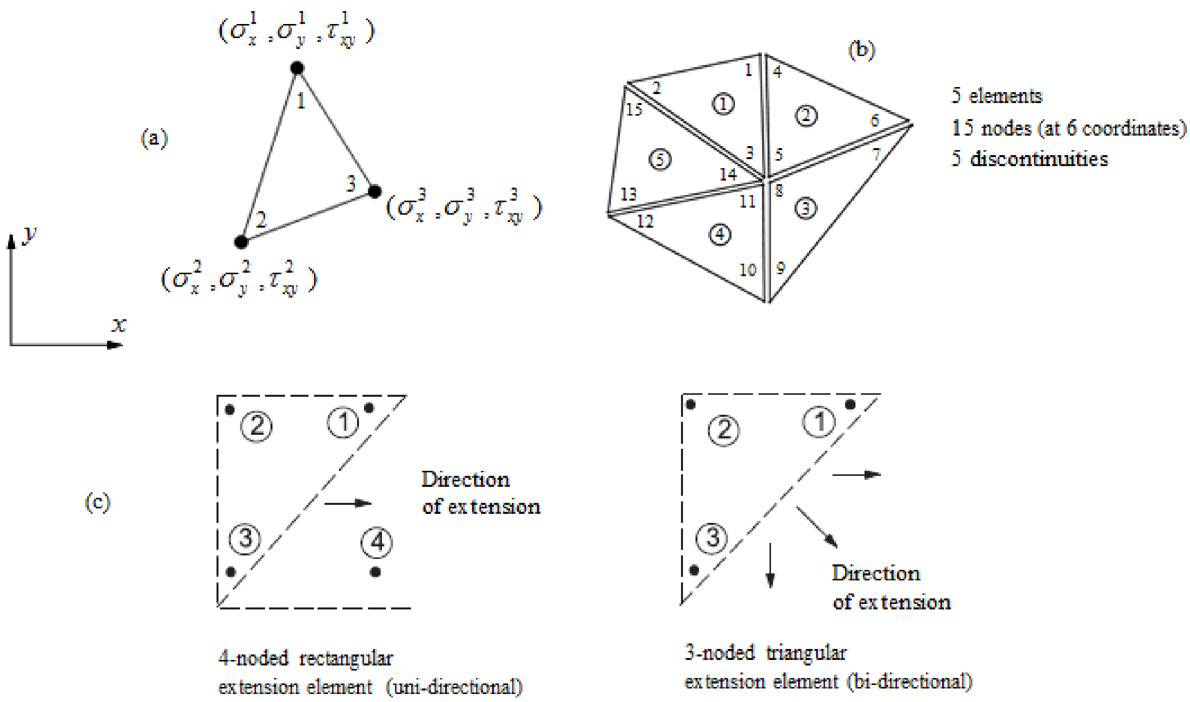

Figure 3. Typical linear triangular element (a), mesh (b) and extension elements (c) used in lower bound analysis

The stresses vary linearly throughout an element according to:

$$\sigma_x = \sum_{l=1}^{3} N_l \, \sigma_x^l \; ; \quad \sigma_y = \sum_{l=1}^{3} N_l \, \sigma_y^l \; ; \quad \tau_{xy} = \sum_{l=1}^{3} N_l \, \tau_{xy}^l \tag{4}$$

where σ_x^l, σ_y^l and τ_{xy}^l are nodal stress components and N_l are linear shape functions. To obtain a rigorous lower bound solution, extension elements are used to extend the statically admissible stress field into a semi-infinite domain. The details of these types of elements can be found in relevant references (Lyamin, 1999; Lyamin & Sloan, 2003).

The Mohr-Coulomb yield criterion in plain strain condition is stated as:

$$F = (\sigma_x - \sigma_y)^2 + (2\tau_{xy})^2 - (2c.\cos\varphi - (\sigma_x + \sigma_y)\sin\varphi)^2 = 0 \tag{5}$$

in which tensile stresses are taken as positive. The equation (4) is the equation of a circle in *X*-*Y* co-ordinate system with center of (0,0) and can be expressed as $X^2 + Y^2 = R^2$ where $X = \sigma_x - \sigma_y$, $Y = 2\tau_{xy}$ and $R = 2c.\cos\varphi - (\sigma_x + \sigma_y)\sin\varphi$. The intrinsically nonlinear Mohr-Coulomb yield function is approximated by an interior equilateral polygon in lower bound limit analysis of this paper. Figure 4 depicts a linearized Mohr-Coulomb yield criterion with *m* sides and *m* vertices. In this study, *m*=36 is adopted for linear approximation of yield function.

Considering equalities and inequalities altogether, the discrete form of lower bound theory can be expressed as:

$$\text{maximize } \mathbf{c}^{\mathrm{T}}\boldsymbol{\sigma}$$

$$\text{subjected to } \begin{cases} \mathbf{A}_1\boldsymbol{\sigma} = \mathbf{b}_1 \\ \mathbf{A}_2\boldsymbol{\sigma} \le \mathbf{b}_2 \end{cases} \tag{6}$$

where c is the vector of objective function coefficients, A_1 is the overall matrix of equality constraints, b_1 is the corresponding right- hand vector of equality equations, A_2 is the overall matrix of inequality constraints, b_2 is the corresponding right- hand vector of inequality constraints and σ is the total vector of unknown stresses.

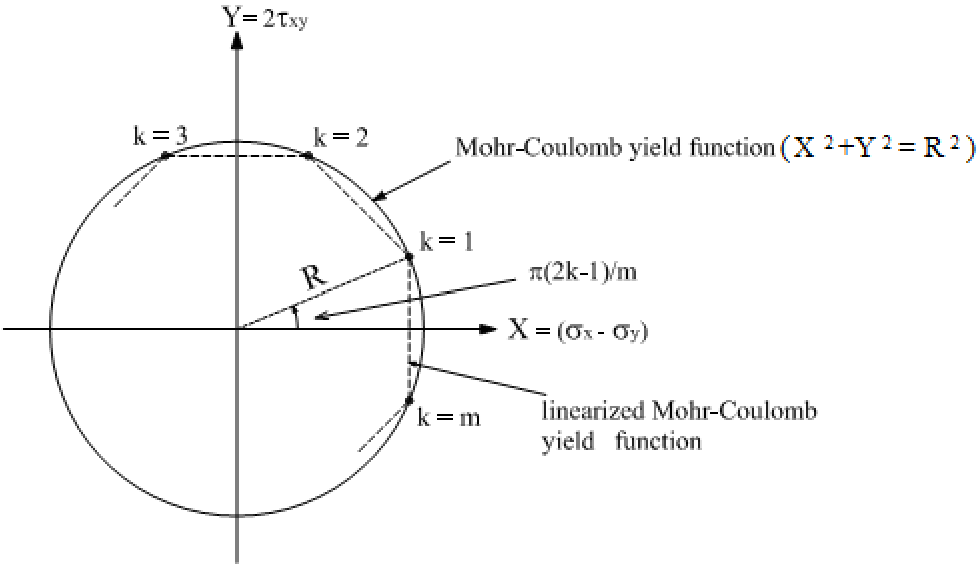

Figure 4. Linearized Mohr-Coulomb yield function

Since all constraints are linear, statement (6) is known as “linear programming” technique in mathematics terminology which can be solve by various algorithms. In this paper, the “interior-point” algorithm has been adopted for solving (optimizing) the finite element form of lower bound analysis. In a separate comparative analyses done by the authors, the “interior-point” algorithm appeared to be faster and more effective than other algorithms such as "simplex" and "active-set" and therefore has been chosen in current study.

In Figure 5, a typical finite element mesh of lower bound method is illustrated in which the known stress boundary conditions and extended stress elements are shown. The mesh is refined around the voids and the footing for better accuracy of results.

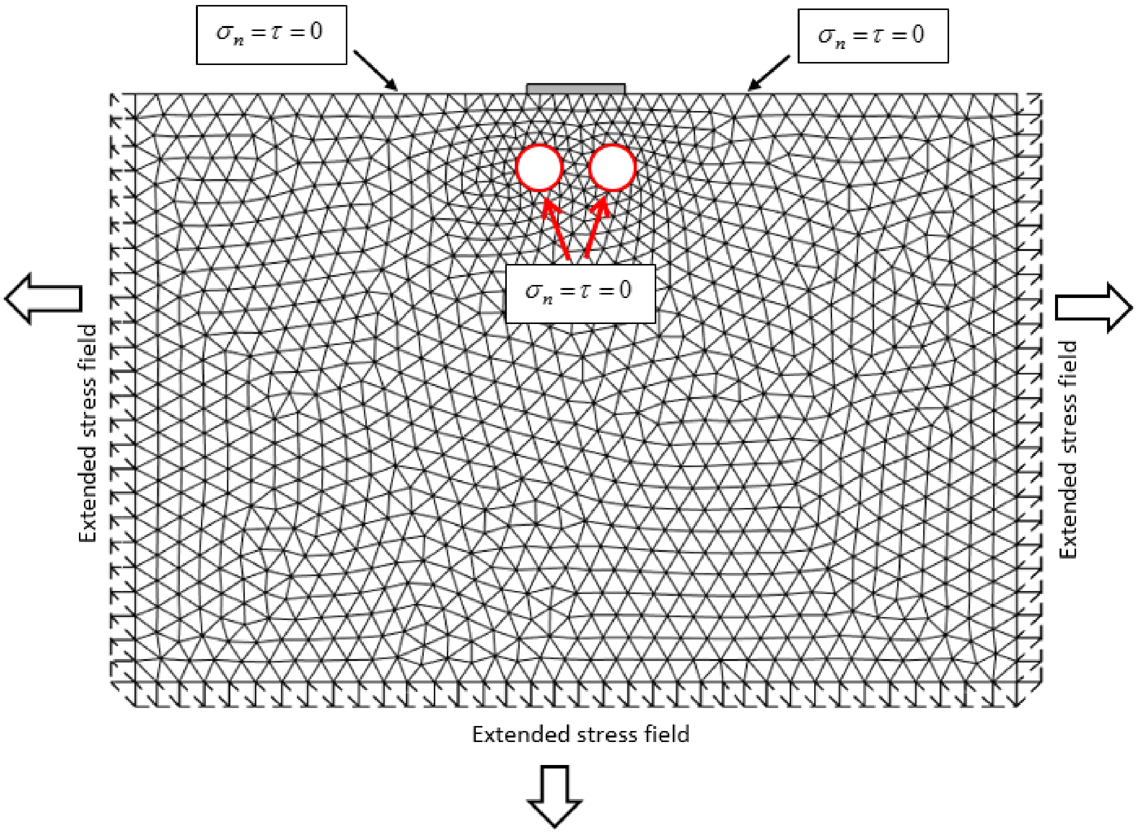

Figure 5. Typical finite element mesh and boundary conditions used in lower bound analysis

4. Results and Discussion

The lower bound limit pressure beneath the strip footing (referred to as '*p*') is regarded as the foundation's bearing capacity situated above the twin voids. Extensive analyses have been conducted across a well-defined set of parameters, and the outcomes have been visually represented through multiple charts. In Figures 6 & 7 dimensionless geometrical parameters include D/B =0.5 , $0.25 \leq d/B \leq 4.5$ and h/B =0.5, 1, 1.5, 3 and soil parameters include $15 \leq c \leq 30$ kPa, $\phi = 30^{\circ}, 35^{\circ}$ are considered in analyses. The relationship between bearing capacity and dimensionless parameters is depicted through pertinent charts and a comparative analysis is performed by contrasting the graph trends with those observed under the assumption of non-existent voids.

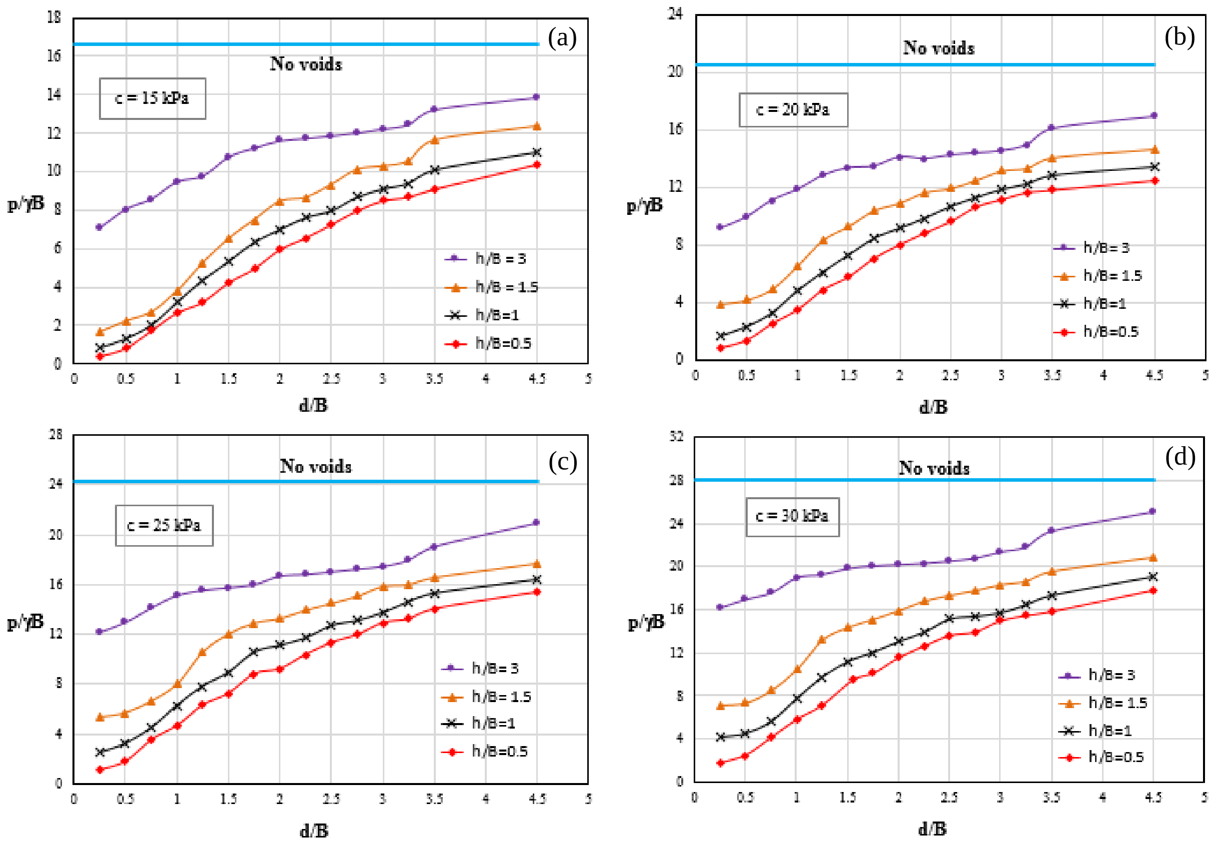

Figure 6. Variation of bearing capacity with geometric parameters and soil cohesion (for ϕ =30°, D/B=0.5)

All of the parameters in Figures 6 & 7 are the same except the internal friction angle which is $\phi = 30°$ for Figure 6 and $\phi = 35°$ for curves of Figure 7. These charts indicate that the presence of voids reduces the bearing capacity of the above footing and by increase of depth and distance of voids from the foundation, this reducing effect diminishes. These figures also demonstrate the influence of soil strength parameters on trend of bearing capacity variation.

For example, in Figure 6a, for d/B=3.5 and h/B=1, the bearing capacity drops about 47 % while this amount is about 38 % for Figure 6b, 35 % for Figure 6c, and 33 % for Figure 6d. This shows that by increasing the cohesion of the soil from 15 to 30 kPa, the bearing capacity increases about 15 % in moderate distance factor (d/B=3.5). For smaller distances, for example when d/B=1, the same trend is observed and in charts of Figure 6a ~ d, the bearing capacity reduction is about 79%, 76%, 73% and 71% respectively. It can be observed that when the two voids are getting close together 3.5 times, the reduction in bearing capacity gets averagely 2 times bigger. The effect of internal friction angle of the soil can be perceived by comparing the corresponding curves of Figures 6 & 7. For instance, in Figure 6b in which $\phi = 30°$,for d/B=2 and h/B=1 the bearing capacity drops about 55 % while this value is 62 % for Figure 7b in which $\phi = 35°$. Also, by comparing the corresponding curves of Figure 6c and Figure 7c for d/B=1 and h/B=1, the bearing capacity decline is 73 % and 78 % respectively. This means that the relative reduction in bearing capacity of soils which are more frictional is bigger than that of less frictional soils. In the other words, although the bearing capacity of a footing above twin voids in more frictional soils is higher, the relative reduction in bearing capacity due to existence of voids is bigger too. Another significant point is that when the voids are very far from each other (maximum 4.5B in this study), the relative decrease in bearing capacity is averagely 33% for $\phi = 30°$ and 40% for $\phi = 35°$. Hence, the decreasing effect of twin voids on bearing capacity is more severe in frictional soils. The effect of voids depth on bearing capacity can also be investigated through comparision of quadruple charts of each graph sets. For instance, in Figure 6b for d/B=2 while depth factor h/B increases from 0.5 to 1, 1.5, and 3, the dimensionless bearing capacity c/γB rises from 8 to 9.2, 10.9, and 14 respectively. For smaller d/B, this trend is more significant. For example, in Figure 7d for d/B=0.5 while depth factor h/B increases from 0.5 to 1, 1.5, and 3 the dimensionless bearing capacity c/γB rises from 2.8 to 5.7, 10.9, and 25.5 respectively.

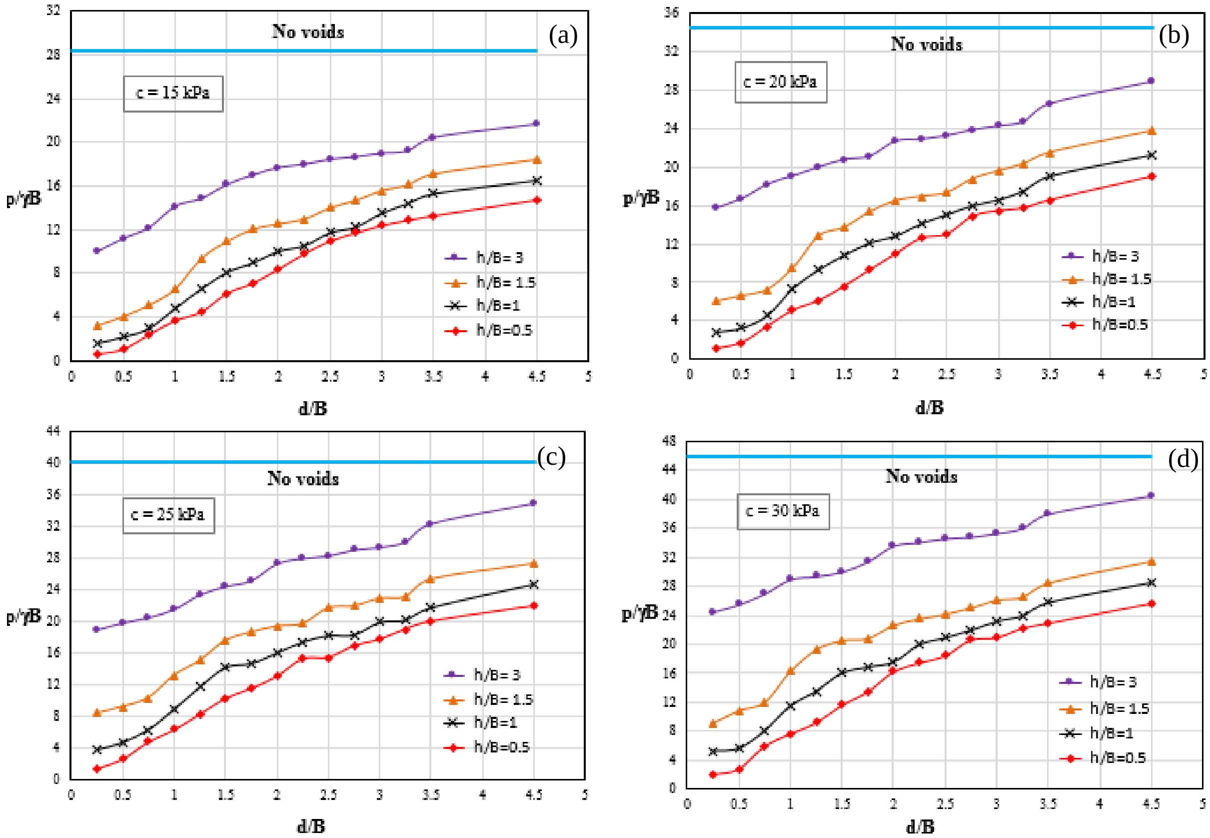

Figure 7. Variation of bearing capacity with geometric parameters and soil cohesion (for ϕ =35°, D/B=0.5)

Further analyses are conducted in the immediate vicinity of the foundation, referred to as foundation scope, precisely within the domain covering the foundation base, with a depth ratio of h/B≤1.5 as illustrated in Figure 8. Any combinations of d and D parameters which satisfy the condition d+2D≤B are feasible for these analyses. However, for graphical representation of the results, geometrical parameters d/B=0.5, D/B=0.25, and h/B=0.25, 0.5, 1, and 1.5 were selected and implemented. Subsequently, the variation of dimensionless bearing capacity of the footing (p/γB) against the dimensionless cohesion parameter of the soil c/ γB=1~8 were plotted, considering soil internal friction angles of ϕ =25°, 30°, 35°, 40° (Figure 9).

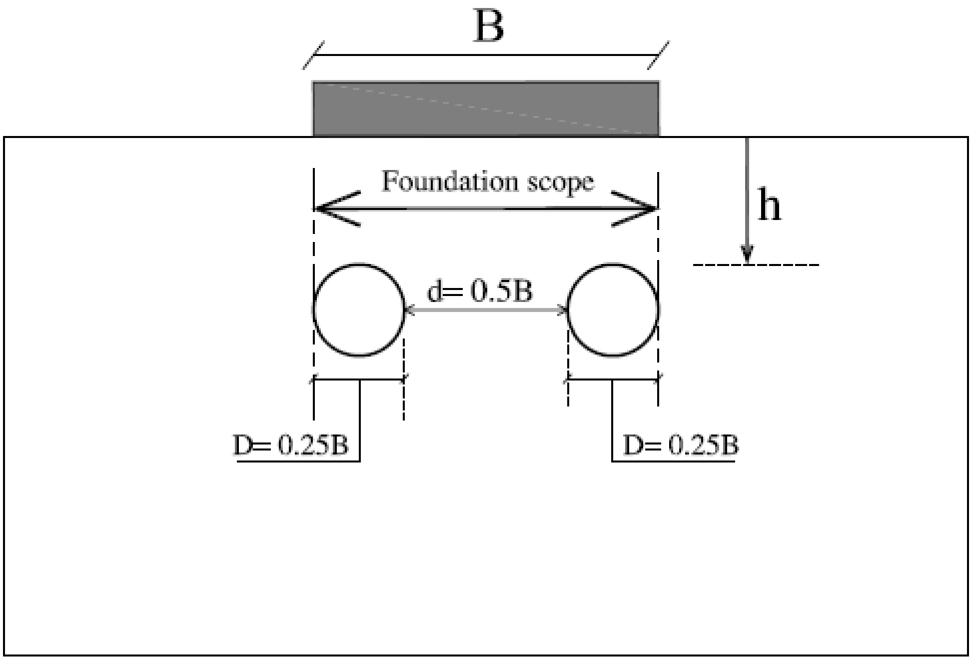

Figure 8. Presence of twin voids within the foundation scope

By referring to the graphs in Figure 9, a clear and natural trend of increasing the bearing capacity of the foundation can be seen with respect to the increase of the cohesion parameter and the internal friction angle of the soil. Also, by increasing the depth of the twin voids, the bearing capacity of the foundation also increases. The remarkable point of these graphs is that the relative increase in bearing capacity is more significant in more frictional soils. For example, in diagram 9-d, when the dimensionless cohesion parameter is $c/\gamma B= 2$, the dimensionless bearing capacity is $p/\gamma B=27.67$, 36.68, 54.21, and 78.53 for ϕ=25°,30°,35°, and 40° respectively. In other words, the relative jump of bearing capacity from ϕ=25° to 30° is roughly 32.5 % while from ϕ=35° to 40° is about 45 %. In the same senario, when dimensionless cohesion parameter reaches to 8, the dimensionless bearing capacity goes to 109.39, 141.07, 211.76, and 298.33 conveys that the relative growth of bearing capacity from ϕ=25° to 30° is roughly 30 % while from ϕ=35° to 40° is about 41 %. Another significant inference from these charts is the influence of voids depth on bearing capacityof the above foundation. For instance, consider a strip footing rested on the cohesive-frictional ground with $c/\gamma B= 4$ and ϕ = 30° with twin voids located in the foundation scope (d/B=0.5 , D/B=0.25). When the depth factor h/B increases from 0.25 to 0.5, 1, and 1.5, the bearing capacity changes approximately from 20 to 29,54, and 79 respectively. For the soil with $c/\gamma B= 5$ and ϕ = 25°, the bearing capacity increase from 21 to 33, 51 , and 69 respectively. This increasing trend is very useful in making the decision of where to bore the infrastructure tunnels. For example, when the twin tunnels of an optical fiber system have to be built beneath a strip footing within the foundation scope (Figure 8), the safety factor of bearing capacity can be enhanced about 50 % by increasing the depth from 0.25B to 0.5B.

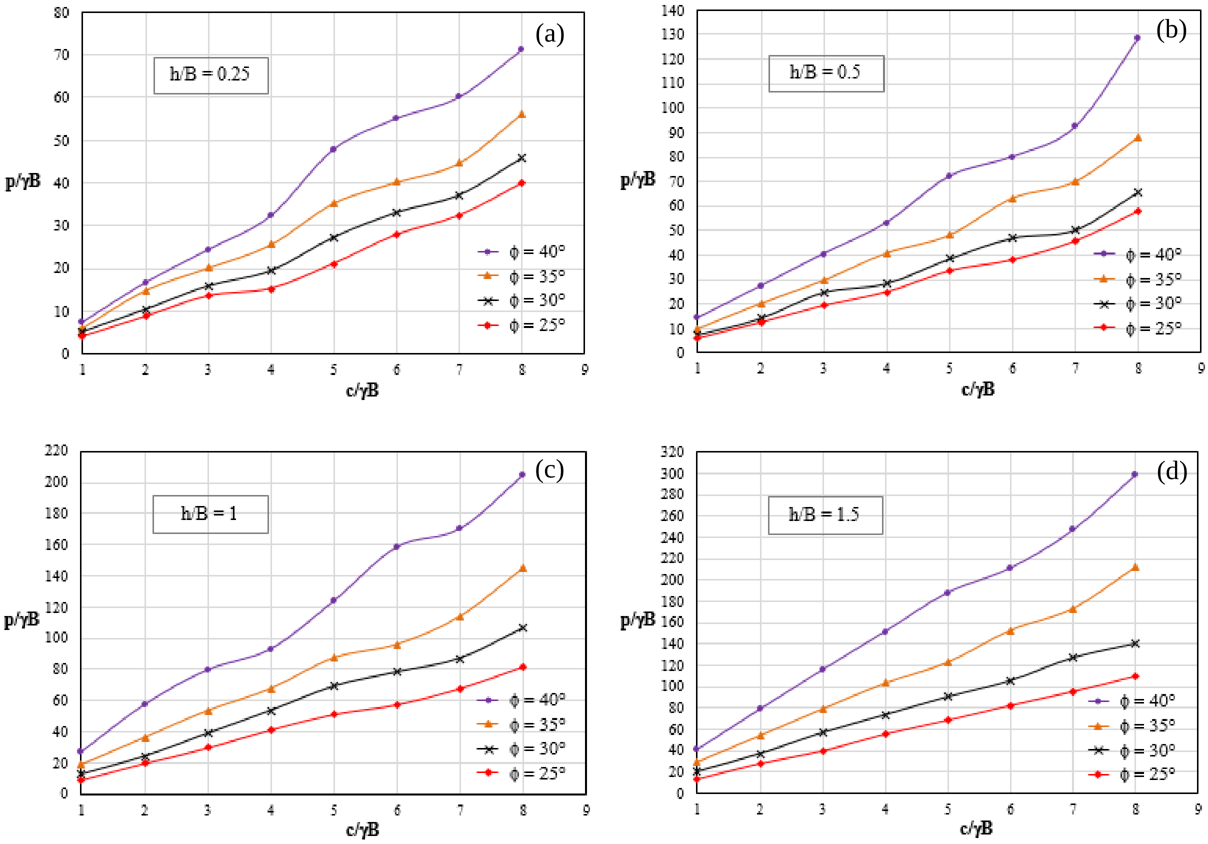

Figure 9. Variation of bearing capacity with depth factor h/B and soil strength parameters (for d/B=0.5, D/B=0.25)

The diagrams in Figures 6 & 7 & 9 demonstrate a clear trend, revealing the influence of soil cohesion, internal friction angle, and voids location on bearing capacity. As a result, these visual representations become valuable tools for geotechnical engineering and the design of underground spaces. The findings provide practical guidance for engineers dealing with varying soil conditions, thereby clarifying the applicability and usefulness of these diagrams in real-world projects.

5. Example of Application

In order to clarify how proposed bearing capacity charts can help engineers to estimate the limit load of strip footings above twin voids, an example is provided here. Consider a twin pipeline tunnels constructed in a cohesive-frictional ground with c=30 kPa, ϕ=30° and γ=20 kN/m^3. The location of the pipeline and the geometry of the problem are illustrated in Figure 10. We have to build a wall which has a foundation width of 1 m on the ground above the pipeline system.

a) Estimate the vertical ultimate load (P) of the wall?

b) Determine the vertical ultimate load (P) when the net distance between the voids (d) dicreases to 0.5 m?

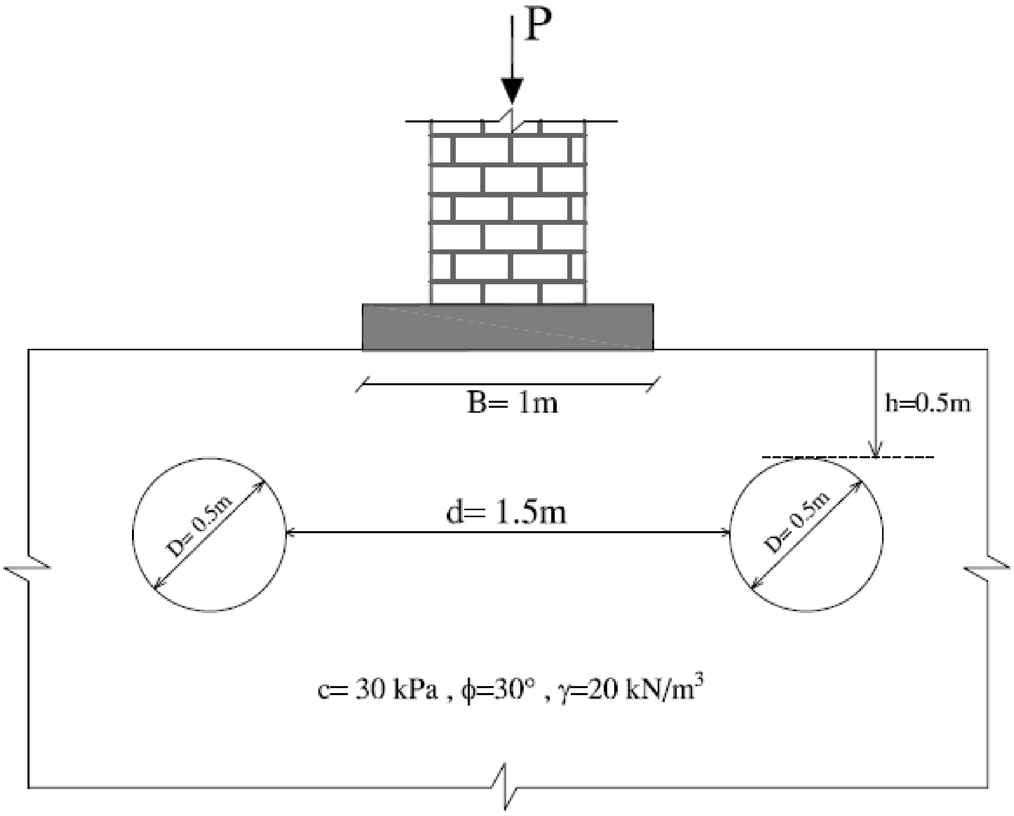

Figure 10. Practical example for determining the ultimate load of the problem

To determine the vertical lower bound load of this system, we should first figure out which graph to use. a) Relevant parameters are as follows:

$$\frac{d}{B}=\frac{1.5}{1}=1.5$$

$$\frac{h}{B}=\frac{0.5}{1}=0.5 \qquad \xrightarrow{Figure\ 6(d)} \frac{p}{\gamma B}=9.5 \quad \Rightarrow p=9.5\gamma B=9.5\times 20\times 1=190\ kPa$$

$$\frac{D}{B}=\frac{0.5}{1}=0.5 \qquad P=p.B=190\times 1=190\ kN/m$$

$$c=30\ \ kPa$$

$$\phi=30^{\circ}$$

Hence, the ultimate load of the wall which can be applied to this voids-foundation system is 190 kN/m along the wall length.

b) When d=0.5 m we must use Figure 6 (d) for d/B=0.5. So we have:

$$\frac{p}{\gamma B}=2.5 \quad \Rightarrow\ p=2.5\gamma B=2.5\times 20\times 1=50\ kPa$$

$$P=\ p.B=50\times 1=50\ \ kN/m$$

The significant effect of voids distance can be observed in this example while the voids come closer three times, the bearing capacity reduces roughly four times.

6. Conclusions

Using the mixed lower bound-finite element method, the investigation of the foundation's bearing capacity in the presence of twin circular voids has revealed crucial insights into the stability of strip footings rested on the cohesive-frictional ground. This study employed dimensionless geometrical parameters such as voids diameter, depth, distance from the foundation centerline alongwith soil parameters include weight, cohesion and internal friction angle to analyze the effects of these factors on lower bound limit load of strip foundations in plane strain condition.

The results demonstrate that the presence of voids substantially reduces the footing's bearing capacity, but this reduction diminishes as voids are located further from the foundation and deeper in the ground. Additionally, soil strength parameters play a significant role, with higher cohesion leading to increased bearing capacity, especially at moderate distances. Comparative analyses between different charts highlight that more frictional soils exhibit higher bearing capacity, but they also experience a greater relative reduction in bearing capacity due to voids. Furthermore, the proximity of the voids to each other significantly impacts bearing capacity reduction. Within the foundation scope (d/B=0.5, D/B=0.25), which is considered as a critical zone beneath the foundation, increasing the dimensionless cohesion parameter and internal friction angle of the soil leads to a general increase in the bearing capacity of the foundation. Moreover, increasing the depth of twin voids increases the bearing capacity remarkably. The relevant graphical representations serve as tools for geotechnical engineering and designing infrastructures.

The charts presented in this study provide practical guidance for engineers and researchers, aiding in the design of underground infrastructures by estimating the lower bound limit load of strip footings in different soil conditions and various twin voids locations within the range of paper's parameters.

References

Azam G., Hsieh, C.W., Wang, M.C.,1991, "Performance of strip footing on stratified Soil deposit with void", Journal of Geotechnical and Geoenvironmental Engineering, vol.117, No.5. https://doi.org/10.1061/(ASCE)0733-9410(1991)117:5(753)

Badie A., ASCE, M. and Wang, M.C., 1984, "Stability of spread footing Above void in clay", Journal of Geotechnical Engineering, Vol. 110, No. 11. https://doi.org/10.1061/(ASCE)0733-9410(1984)110:11(1591)

Chen WF. Limit Analysis and Soil Plasticity. Developments in Geotechnical Engineering, vol. 7. Elsevier: Amsterdam, 1975.

Joon Kyu Lee, Sangseom Jeong, Junyoung Ko, 2014," Undrained stability of surface strip footings above voids", Computer and Geomechanics 62,128-135. https://doi.org/10.1016/j.compgeo.2014.07.009

Kiyosumi, M., Kusakabe, O. and Ohuchi, M., 2007, "Yielding pressure of spread footing above multiple voids", Journal of Geotechnical and Geoenvironmental Engineering,133: 1522 – 1531. https://doi.org/10.1061/(ASCE)1090-0241(2007)133:12(1522)

Kiyosumi, M., Kusakabe, O. and Ohuchi, M., 2011," Model tests and analyses of bearing capacity of strip footing on stiff ground with voids", Journal of Geotechnical and Geoenvironmental Engineering, 137: 363 – 375. https://doi.org/10.1061/(ASCE)GT.1943-5606.0000440

Lyamin, A. V. (1999). “Three-dimensional lower bound limit analysis using nonlinear programming.” Ph.D. Thesis, Univ. of Newcastle, Australia.

Lyamin, A. V., and Sloan, S.W. (2002). “Lower bound limit analysis using non-linear programming.” Int. J. Numer. Methods Eng., 55, 573–611. https://doi.org/10.1002/nme.511

Lyamin, A. V., and Sloan, S.W. (2003). “Mesh generation for lower bound limit analysis.” Elsevier Science, Int. J. Advances in engineering software, 34, 321–338. https://doi.org/10.1016/S0965-9978(03)00032-2

Naveen James and K. Ramu, 2017, “Effect of twin tunnel construction on existing buildings supported on piled foundations”, International Journal of Geotechnical Engineering, Vol. 11, Issue 4.

Sabouni R., 2013, “Displacement and effective stresses changes underneath strip footing on stiff ground with single and double voids”. Geo Montreal. http://dx.doi.org/10.13140/2.1.1334.1447

Sloan, S. W. 1988, “Lower bound limit analysis using finite elements and linear programming”, Int. J. Numer. Anal. Methods Geomech., 12,61–67.

Sireesh, S., Sitharam, T.G., Dash, S.K. 2009, “Bearing capacity of circular footing on geocell-sand matterss overlaying clay bed with void”, Geotextiles and Geomembranes, 27: 89 - 98. https://doi.org/10.1016/J.GEOTEXMEM.2008.09.005

Thomas C. Kinney., and Billy Connor., 1987, “Geosynthetics supporting embankments over Voids”, Journal of Cold Regions Engineering, Vol. 1, No. 4. https://doi.org/10.1061/(ASCE)0887-381X(1987)1:4(158)

Wang, M. C., Hsieh, C.W., 1987, “Collapse load of strip footing above circular void”, ASCE, Journal of Geotechnical Engineering, Vol. 113, Issue 5. https://doi.org/10.1061/(ASCE)0733-9410(1987)113:5(511)

Wilson, D., Abbo, A., Sloan, S., and Lyamin, A. (2014), "Undrained Stability of Dual Circular Tunnels." Int. J. Geomech., 10.1061/(ASCE)GM.1943-5622.0000288, 69-79. http://doi.org/10.13140/2.1.1751.8726

Yan-Jun Sun, Shao-Wei Zhu, and Peng-Yun Wu 2019, "Effects of twin tunnels on existing building foundations: Case study of Guanyinqiao subway station, Chongqing". Journal of Central South University, Vol. 26, Issue 7.